

# Charge transfer in TATB and HMX under extreme conditions

Chaoyang Zhang · Yu Ma · Daojian Jiang

Received: 31 January 2012 / Accepted: 23 May 2012 / Published online: 16 June 2012  
© Springer-Verlag 2012

**Abstract** Charge transfer is usually accompanied by structural changes in materials under different conditions. However, the charge transfer in energetic materials that are subjected to extreme conditions has seldom been explored by researchers. In the work described here, the charge transfer in single molecules and unit cells of the explosives TATB and HMX under high temperatures and high pressures was investigated by performing static and dynamic calculations using three DFT methods, including the PWC functional of LDA, and the BLYP and PBE functionals of GGA. The results showed that negative charge is transferred from the nitro groups of molecular or crystalline TATB and HMX when they are heated. All DFT calculations for the compressed TATB unit cell indicate that, generally, negative charge transfer occurs to its nitro groups as the compression increases. PWC and PBE calculations for crystalline HMX show that negative charge is first transferred to the nitro groups but, as the compression increases, the negative charge is transferred from the nitro groups. However, the BLYP calculations indicated that there was gradual negative charge transfer to the nitro groups of HMX, similar to the case for TATB. The unrelaxed state of the uniformly compressed TATB causes negative charge to be transferred from its nitro groups, in contrast to what is seen in the relaxed state. Charge transfer in TATB is predicted to occur much more easily than in HMX.

**Keywords** Charge transfer · Explosives · Extreme conditions

## Introduction

Much attention is currently being paid to the structures, properties, and behaviors of materials subjected to extreme conditions, such as high temperatures, high pressures, high densities, intense radiation, strong electric fields, high shock or impact velocities, and so on. For example, LANL is currently sponsoring the MaRIE (matter–radiation interactions in extremes) Project, which focuses on the interactions between materials and radiation under extreme conditions [1].

Energetic materials (EMs) are a group of special materials that detonate and combust. The behavior of EMs under extreme conditions like high temperatures and high pressures has attracted the attention of researchers, as detailed descriptions of their electronic structures, geometries, and chemical reaction mechanisms are essential if we are to understand the events that happen at their reactive fronts under the conditions associated with detonation or combustion. Under shock conditions, EMs can be heated to over 3000 °C and subjected to a compression of several tens of GPa, leading to a reduction in volume of about 30 %. Their electronic structures, geometries, and chemical reactivities can change considerably under these extreme conditions when compared to those seen under ambient conditions.

Charge transfer is an inevitable consequence of the changes in electronic structures that occur under extreme conditions. However, to our knowledge, reports in the literature on this topic for EMs are scarce. We therefore decided to explore this area of research, and we are reporting the results of our study in this work. We employed molecular simulations to elucidate the charge transfer in gaseous and perfectly crystalline 1,3,5-triamino-2,4,6-trinitrobenzene (TATB) and 1,3,5,7-tetranitro-1,3,5,7-octahydrotriazocine (HMX) under conditions that became extreme, like high

C. Zhang (✉) · Y. Ma · D. Jiang  
Institute of Chemical Materials, China Academy of Engineering  
Physics (CAEP),  
P.O. Box 919-327, Mianyang, Sichuan, China 621900  
e-mail: zcy19710915@yahoo.com.cn

temperatures and high pressures. TATB is a well-known and rather insensitive explosive, and HMX is called the “king of explosives,” as it is extensively applied as an energetic component in many propellant and explosive formulations, due to its excellent performance in this context.

Molecular simulations based on quantum chemistry (QC), molecular mechanics (MM), molecular dynamics (MD), molecular reaction force field (MRF), Monte Carlo (MC), and mesoscale calculations are becoming an increasingly important tool for exploring the structures, properties, and behavior of materials, in particular EMs under extreme conditions, due to high-risk, rapid, and complex nature of their decomposition, which make experimental studies of these substances rather difficult.

We first provide a brief review of existing molecular simulation results obtained for EMs under extreme conditions, which were helpful in our study. Periodic calculations based on force field or DFT methods were used to study the static behaviors of explosives at high pressures, including under hydrostatic, uniform, and uniaxial compression. For instance, the force field potential energy function CHARMM29 was employed to study 1,3-diamino-2,4,6-trinitrobenzene (DATB), which has a similar molecular structure to TATB, at high pressures [2]. Wu et al. carried out DFT and configuration interaction calculations to examine the insulator-to-metal transition of the energetic crystalline solid TATB. They predicted that the lower bound for the metallization pressure was 120 GPa, and therefore concluded that electronic excitation is not involved in the primary stages of detonation for a defect-free TATB crystal [3]. Later, a combined DFT and MD method (also called *ab initio* MD) was devised, and this was soon applied to investigate the dynamic behaviors of explosives at high temperatures and high pressures, as well as shock velocities (loaded if necessary). Manaa et al. reported the first quantum-based multiscale simulations to study the reactivity of shocked perfect crystals of TATB, and found that high concentrations of nitrogen-rich heterocyclic clusters occur when TATB experiences overdriven shock speeds of 9 km/s for up to 0.43 ns and 10 km/s for up to 0.2 ns [4]. Another similar simulation was performed by them for crystalline HMX at a density of 1.9 g/cm<sup>3</sup> and 3500 K: conditions roughly similar to the Chapman–Jouguet detonation state. They estimated reaction rates for the products H<sub>2</sub>O, N<sub>2</sub>, CO<sub>2</sub>, and CO of 0.48, 0.08, 0.05, and 0.11 ps<sup>-1</sup>, respectively [5]. Wei et al. carried out Car–Parrinello molecular dynamics (CPMD) simulations to investigate the thermal decomposition of solid nitromethane (NM). They found that it undergoes chemical decomposition at about 2200 K under ambient pressure. Reaction initiation involves both proton transfer and C–N bond cleavage, and the final products are H<sub>2</sub>O, CO<sub>2</sub>, N<sub>2</sub>, and CNCNC [6]. Because of the long simulation times involved, the number of molecules that can be simulated is very

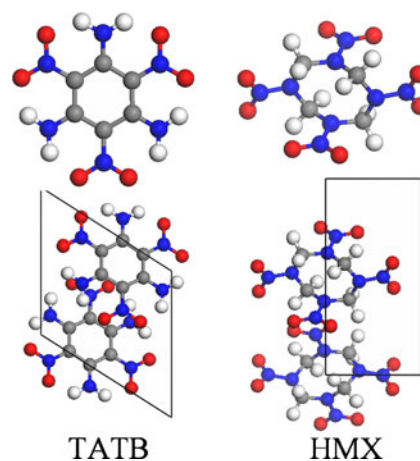


**Fig. 1** Single molecules and unit cells of TATB and HMX. C, H, N and O atoms are shown in *gray*, *white*, *blue*, and *red*, respectively

limited, and it is impossible for a group with only moderate computational resources to perform such simulations over a short period.

A forcefield with bond order functions—called the molecular reactive force field (MRF)—has recently been used to explore the events that occur under extreme conditions. More than one million atoms can be included such simulations. Therefore, the biggest advantage of the MRF method is that it can deal with much larger systems that are much closer to real systems than an *ab initio* MD method can. Strachan et al. extended the MRF ReaxFF to describe the high-energy nitramine 1,3,5-trinitro-1,3,5-hexahydrotriazine (RDX), and used this MRF to study the shock-induced chemistry of RDX. They found that for high impact velocities (>6 km/s), RDX molecules decompose and react to form a variety of small molecules over very short timescales (<3 ps). The products of this reaction are consistent with those found experimentally at longer timescales [7]. Furnish et al. compared the decomposition reactions of pure RDX and

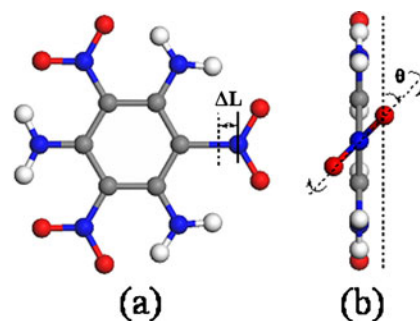


**Fig. 2** Model used to perform calculations for a TATB molecule: the stretching of the C–N bond in a nitro group (a) and the torsion of a nitro group out of the plane of the benzene ring (b)

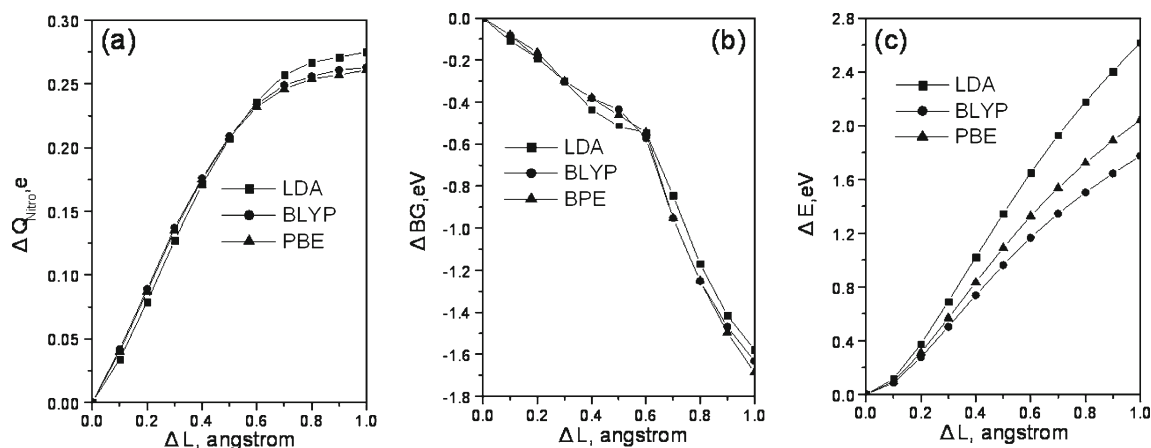


**Fig. 3** Plots of the change in the length of the C–N bond ( $\Delta L$ ) versus the change in the charge on the stretched nitro group (a; in units of the charge on the electron,  $e$ ), the change in the band gap (b), and the change in the total energy (c) of the TATB molecule, respectively

the mixture RDX/Estane and found that the delay time increased after adding Estane [8]. Another interesting finding was obtained by performing ReaxFF simulations on RDX with a void. As the void collapsed, two distinct reaction regimes were observed. From the arrival of the shock wave until the closure of the void 2.6 ps later, rapid production of  $\text{NO}_2$  was observed. Shortly after that, when molecules hit the wall downstream after 2.6–3.9 ps, various chemical products such as  $\text{N}_2$ ,  $\text{H}_2\text{O}$ , and HONO were produced [9]. This method was also applied to re-examine the anisotropic sensitivities of the crystal faces of pentaerythritol tetranitrate (PETN). A higher rate of temperature increase and the formation of the product with the (110) face rather than the (100) face confirmed that the (110) face is more sensitive, in good agreement with previous experimental results [10]. Additionally, a large carbon cluster was observed in an MRF simulation of TATB [11], as mentioned above for

ab initio MD simulations [4]. Empirical force field calculations were carried out to explore the molecular dynamics of the void defects in crystalline RDX [12].

Based on the brief survey provided above, we can see that molecular simulation is a useful way to elucidate the structures, properties, and behaviors of EMs under extreme conditions. Some of the results obtained from these simulations are found to be highly consistent with experiments, while others are novel and can provide useful information for understanding the events associated with EMs under extreme conditions. We also find that charge transfer should be inevitable under conditions that become extreme. In the work described in this paper, we focused on charge transfer in TATB and HMX under conditions that ranged from the usual to high pressures or high temperatures. Hopefully, our work will help to expand knowledge of both charge transfer [13, 14] and EMs.

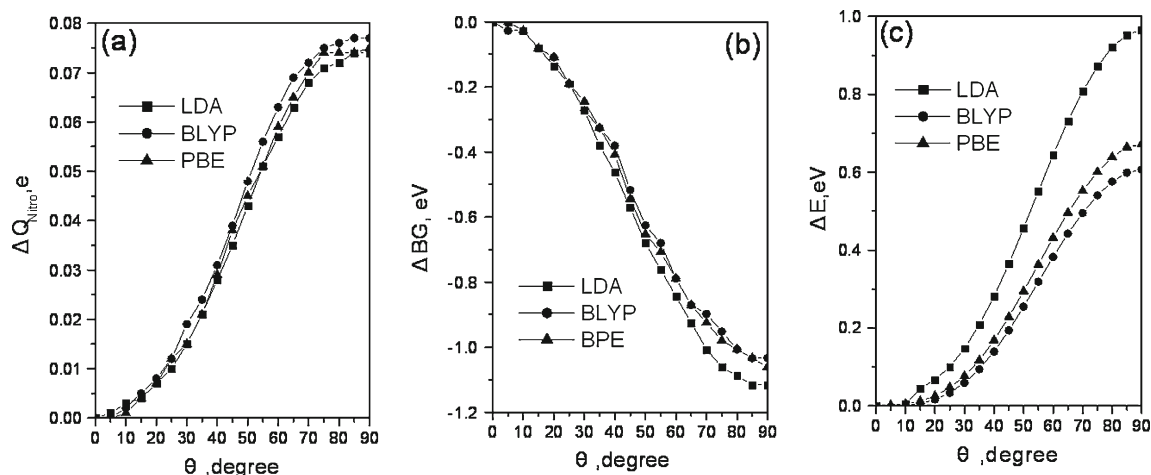


**Fig. 4** Plots of the rotation angle ( $\theta$ ) of the nitro group versus the change in the charge on the nitro group (a; in units of the charge on the electron,  $e$ ), the change in the band gap (b), and the change in the total energy (c) of the TATB molecule, respectively

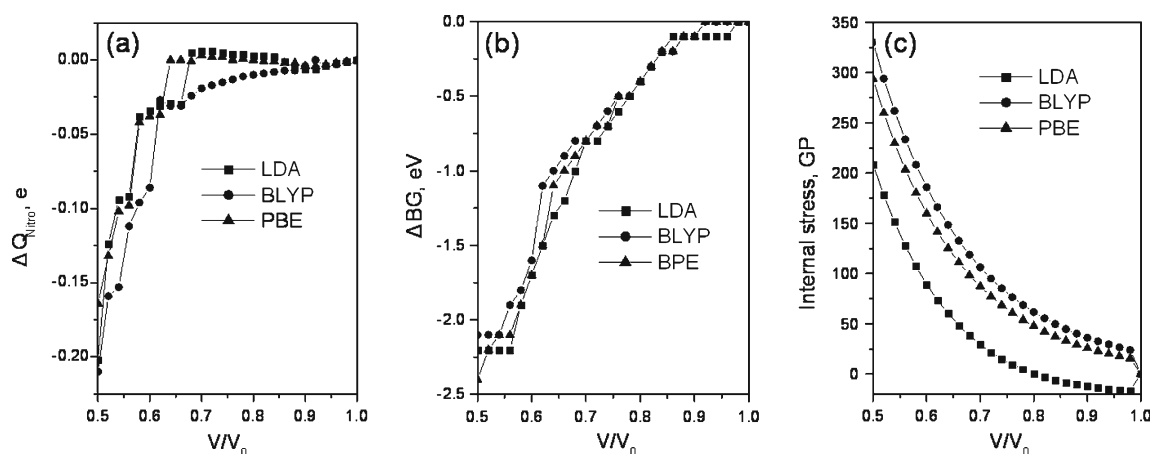


**Fig. 5** Plot of the volume strain ( $V/V_0$ ) versus the change in the charge on the nitro group (a; in units of the charge on the electron,  $e$ ), the change in the band gap (b), and the internal stress (c) during the uniform compression of the TATB unit cell, respectively

## Methodology

The static and dynamic behaviors of TATB and HMX (the molecular structures and unit cells of which are shown in Fig. 1) at high pressures or high temperatures were considered in this work. A nitro group in an organic compound is usually an electron acceptor and an ignition group; breaking the bond between the nitro group and the molecule initiates the molecular decomposition. The charge on a nitro group can quantitatively reflect its chemical environment. Obviously, change in the amount of charge on the nitro group denotes the change in its chemical environment. In other words, the changes in the chemical environment induced by extreme conditions can be represented by the change in the amount of charge transferred. In this work, the charge transfer was denoted by the change in the Mulliken charge ( $\Delta Q_{\text{nitro}}$ ) of a given nitro group, or by the average  $\Delta Q_{\text{nitro}}$  value for all nitro groups in a molecule (to get a sense of the average charge transfer, as there are three nitro groups in a

TATB molecule and four nitro groups in an HMX molecule). Because charge transfer is basically electron transfer, some of the characteristics associated with electronic structures, such as the band gap (BG), LUMO and HOMO, and density of states (DOS), were given out conditionally for a comprehensive understanding on it. This approach can overcome the problems associated with analyzing charge transfer based on atomic charges. As is well-known, Mulliken charges depend strongly on the calculation method employed including functionals and basis sets. In the case of compression, internal stress was calculated using the equation  $P = \Delta E / \Delta V$ . Detailed modeling and calculations were carried out as follows:

- (1) Elongate the C–N bond of the nitro group or twist it out of the plane of the benzene ring of a TATB molecule to mimic a gaseous TATB molecule that is being subjected to a high temperature. Three DFT methods—LDA/PWC, BLYP, and PBE—were adopted to fully optimize the TATB molecule or to optimize it with fixed C–N bond lengths ( $L$ ) or torsion angles ( $\theta$ ). As illustrated in Fig. 2,  $\Delta L$  is the increase in the C–N bond length (in increments of 0.1 Å) relative to that of the fully optimized

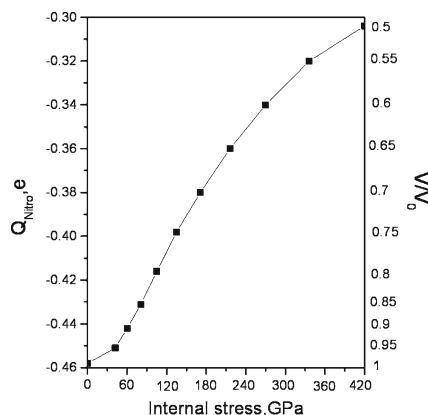


**Fig. 6** Plot of  $Q_{\text{nitro}}$  and  $V/V_0$  against the internal stress in compressed, unrelaxed TATB

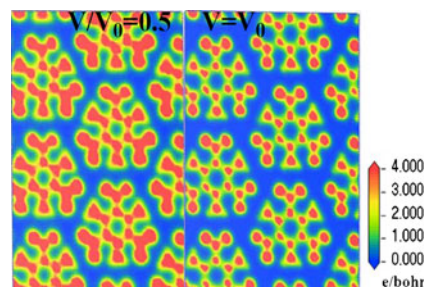


**Fig. 7** Comparison of the electron densities in TATB under high (left) and normal (right) pressure



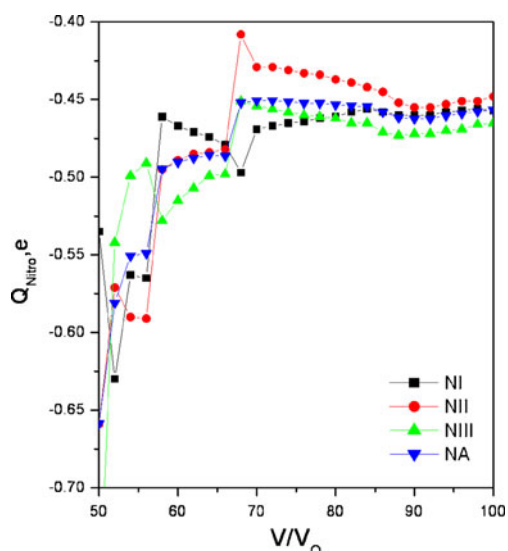


**Fig. 8** Plot of  $V/V_0$  versus  $Q_{\text{Nitro},e}$  for the three nitro groups (NI, NII, and NIII) in TATB, and for an “average” nitro group (NA; i.e., the values for NI, NII, and NIII were averaged)

TATB molecule; while  $\theta$ , the torsion angle, was increased from zero (for the fully optimized TATB molecule) to  $90^\circ$  in steps of  $5^\circ$ .

- (2) Uniformly compress the unit cells of the TATB and HMX crystals to  $V/V_0=50\%$  in steps of  $2\%$  to mimic perfectly crystalline TATB and HMX at high pressure. The abovementioned DFT methods were also employed to relax the atomic positions with fixed lattice parameters.
- (3) Subject single gaseous molecules and the unit cells of TATB and HMX, respectively, to temperatures of 1000, 2000, and 3000 K and carry out ab initio MD simulations with  $NVT$  ensembles to study their dynamic behaviors at high temperatures. In these cases, the LDA/PWC functional [15], the massive GGM

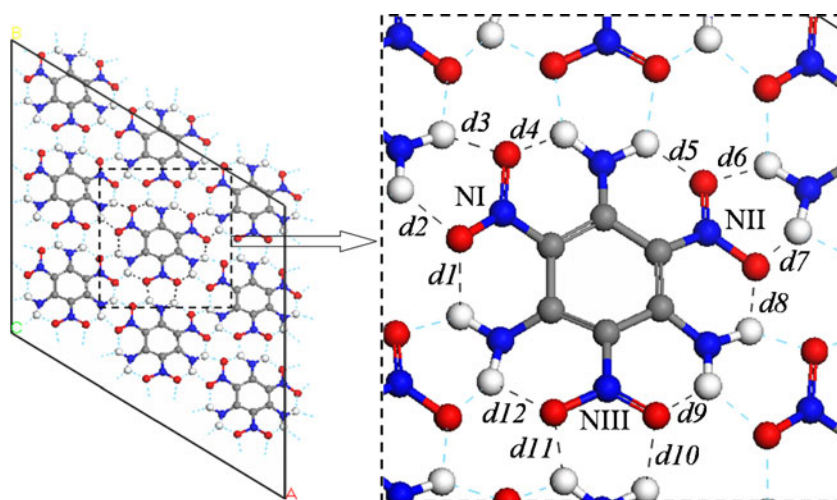
thermostat [16], and the velocity Verlet integration algorithm [17] were applied in simulations that lasted for 1 ps for the single molecules and 5 ps for the unit cells and used time steps of 0.5 fs. We then randomly selected some balanced structures at different temperatures and recalculated their electronic structures without relaxation to study the charge transfer.

For a single explosive organic molecule, a common DFT method can be used to obtain an accurate geometry and electronic structure; for an organic crystal, current DFT methods have been shown to poorly describe van de Waals forces. However, we have to choose them to study TATB and HMX crystals because no other better method is available. For example, Byrd and Rice used three DFT methods (PW91, PBE, and LDA) to calculate crystal structures for five molecular crystals of high-energy materials over a range of experimental pressures, including HMX, RDX, 2,4,6,8,10,12-hexanitrohexaazaisowurzitane (CL-20), TATB, and PETN. They found that both PW91 and PBE generally overestimate volumes relative to experimental values, while LDA underestimates crystal volumes when compared to experimental values. However, these inaccuracies diminish as the pressures increases [18, 19]. Besides, all of the ab initio boundary calculations in the reports mentioned in the “Introduction” are DFT calculations. Similarly, three DFT methods (LDA/PWC, BLYP, and PBE) were selected for this work. All calculations were carried out using the DFT-based package Dmol<sup>3</sup> [20–22].

## Results and discussion

We regard the results from the ab initio MD simulations as the results obtained under dynamic conditions, and the

**Fig. 9**  $3 \times 3 \times 1$  supercell of TATB, extending from its compressed unit cell. **a** Top view of the (001) face, **b** numbering scheme for interatomic bonds in the center molecule, and **c** side view along the  $b$  axis



others as the results obtained under static conditions. We discuss these two sets of results separately in the following two sections.

### Static conditions

We first focus on the static results for a TATB molecule. In this case, one of its nitro groups is stretched along the C–N bond of the nitro group, or is twisted out of the benzene ring with a fixed C–N bond length (derived from the full optimization of the molecule), which could occur because the TATB molecule is being subjected to extreme temperatures. During the stretching, negative charge is transferred from the nitro group, as shown in Fig. 3a, and tend to zero when the bond is broken. Actually, a neutral NO<sub>2</sub> molecule is without net charges. When the bond breaks, producing two radicals, the band gap (BG) decreases and total energy increases, as illustrated in Fig. 3b and c, respectively. As indicated in Fig. 3, the three DFT methods give the same variations in  $\Delta Q_{\text{nitro}}$ ,  $\Delta \text{BG}$ , and  $\Delta E$  (change in total energy) during the stretching, but there are some differences in the calculated relative values. For instance, using LDA leads to the biggest increase in  $\Delta Q_{\text{nitro}}$  transferred and the total energy, and the smallest decrease in  $\Delta \text{BG}$ ; the variations in  $\Delta Q_{\text{nitro}}$  and  $\Delta \text{BG}$  derived using the two GGA methods (BPE and BLYP) are very similar, but they both show greater differences from those obtained using LDA. The three methods give very different dissociation energies (BDEs) for the C–N bond of the bond: the largest value is given by LDA, and the smallest is given by BLYP.

The three methods also give the same variations in the above parameters as the C–N bond of the nitro group is rotated, as illustrated in Fig. 4. As the nitro group deviates further and further from the plane of the benzene ring,  $\Delta Q_{\text{nitro}}$  increases,  $\Delta \text{BG}$  decreases, and  $\Delta E$  increases. A previous study showed there is a correlation between the  $Q_{\text{nitro}}$  values and the impact sensitivities of nitro compounds: as  $Q_{\text{nitro}}$  becomes increasingly negative, the impact sensitivity decreases [23]. This correlation is based on the fact that an increasingly negative  $Q_{\text{nitro}}$  leads to a more stable nitro compound. Here, both stretching and twisting cause the stability of the TATB molecule to decrease, as  $Q_{\text{nitro}}$  becomes increasingly negative, BG decreases, and the total energy increases. In other words, all of these indicators of molecular stability change in a consistent manner.

Based on the above discussion, we can see that stretching or twisting a nitro group in a TATB molecule causes the transfer of some electrons from the nitro group, and decreases its negative charge, indicating that some negative charge is transferred from the electron acceptors (the nitro groups) in the TATB molecule at high temperatures.

Next, we consider the charge transfer in the unit cells of TATB and HMX when they are uniformly compressed.

**Table 1** Charges on the nitro groups NI–NIII ( $Q_{\text{NI}}$ – $Q_{\text{NIII}}$ ) and interatomic distances ( $d\text{I}$ – $d\text{I2}$ ) in TATB, according to LDA calculations. For a guide to  $d\text{I}$ – $d\text{I2}$ , see Fig. 8b

V/V <sub>0</sub>	$Q_{\text{NI}}$	$Q_{\text{NII}}$	$Q_{\text{NIII}}$	$d\text{I}$	$d\text{II}$	$d\text{III}$	$d\text{I}$	$d\text{2}$	$d\text{3}$	$d\text{4}$	$d\text{5}$	$d\text{6}$	$d\text{7}$	$d\text{8}$	$d\text{9}$	$d\text{10}$	$d\text{11}$	$d\text{12}$
0.70	-0.469	-0.429	-0.454	1.344	1.348	1.346	1.571	1.842	1.741	1.839	1.784	2.055	1.553	1.633	1.587	1.903	1.586	1.704
0.68	-0.497	-0.408	-0.451	1.333	1.345	1.343	1.585	1.735	1.684	1.797	1.914	2.028	1.516	1.665	1.620	1.970	1.630	1.814
0.66	-0.479	-0.482	-0.498	1.323	1.330	1.334	1.901	1.666	1.484	1.672	1.605	1.674	1.510	1.707	1.641	1.820	1.515	1.741
0.64	-0.474	-0.484	-0.499	1.316	1.324	1.328	1.960	1.645	1.459	1.664	1.601	1.684	1.469	1.699	1.634	1.783	1.492	1.749

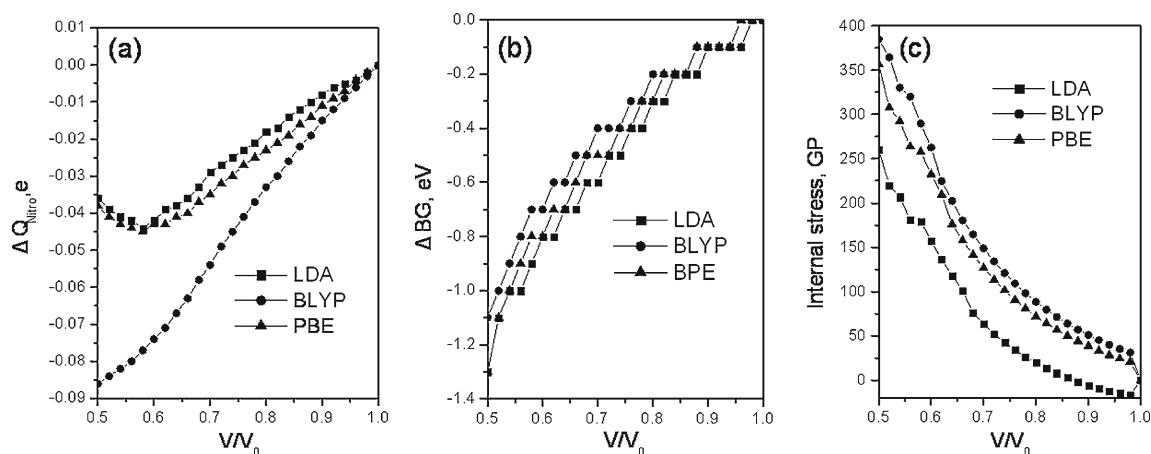


**Fig. 10** Plots of the volume strain ( $V/V_0$ ) versus the change in the charge on the nitro group (**a**; in units of the charge on the electron,  $e$ ), the change in the band gap (**b**), and the internal stress (**c**) for the HMX unit cell, respectively

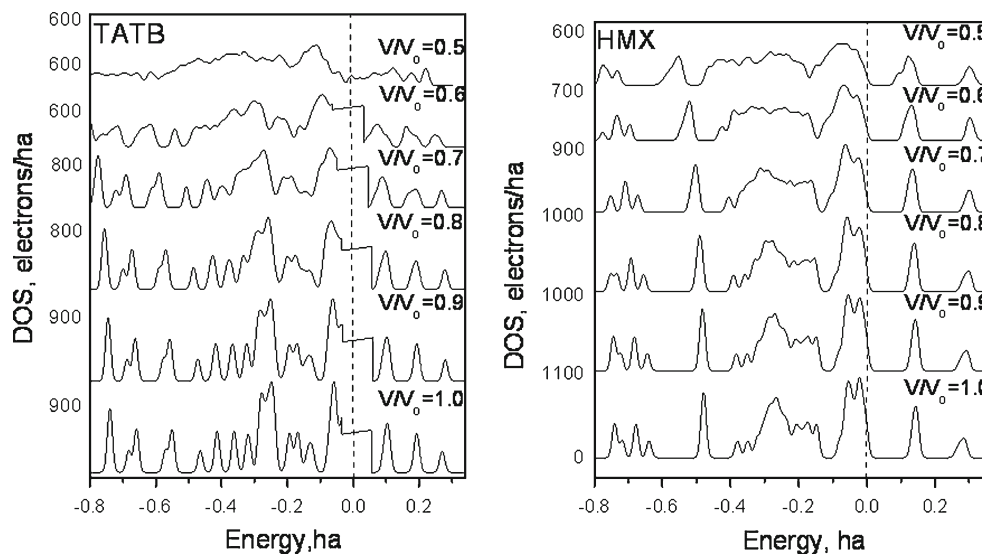
Figure 5a shows the variation in  $\Delta Q_{\text{nitro}}$  in the unit cell of the TATB molecule as it is compressed. However, the corresponding variations given by LDA and PBE differ from that given by BLYP. When LDA and PBE are used,  $\Delta Q_{\text{nitro}}$  is found to initially decrease with some fluctuations, before decreasing rapidly; when BLYP is used,  $\Delta Q_{\text{nitro}}$  initially gradually decreases, with a local maximum occurring at  $V/V_0=0.92$ .

We believe that the amount and the sign of the charge transferred are determined by the relative positions of atoms in the cell. To examine this, we first carried out BLYP calculations for the electronic structures of uniformly compressed and unrelaxed TATB as an extreme case, which resembles the case when there is insufficient time for the compressed TATB to relax. As a result, we observed reverse charge transfer in Fig. 6, in contrast to the results seen in Fig. 5a. As illustrated in Fig. 7, the electron densities are

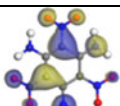
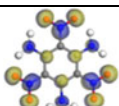
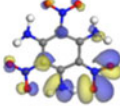
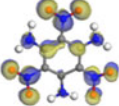
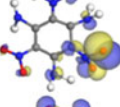
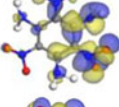
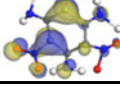
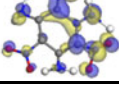
averaged or delocalized, and they increase after compression. The nitro groups increase in electron density to a lesser degree than the other atoms, causing negative charge to be transferred from the nitro groups. Kuklja et al. calculated the electronic structures of solid and unrelaxed FOX-7 and found that the BG is much larger for relaxed FOX-7 [24]. That is, the unrelaxed state causes the electrons to become more delocalized. It also shows that the uniform shortening of interatomic distances in the TATB unit cell upon compression prompts negative charge transfer from the nitro groups.

We were also interested in the interatomic distances in the compressed and the relaxed unit cell. In this case, the results of the LDA calculations were chosen for analyses. As shown in Fig. 8, the negative charge on each of the three nitro groups of TATB gradually increases, albeit with some fluctuations. Now, numbering the nitro groups and interatomic

**Fig. 11** DOSs for the TATB and HMX unit cells under different volume strains ( $V/V_0$ )



**Table 2** Distributions of frontier orbitals, energy gaps, relative energies, and the changes in the average charge on a nitro group in an *NVT*-balanced TATB molecule at different temperatures

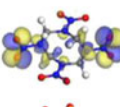
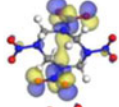
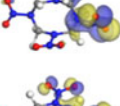
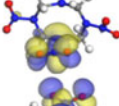
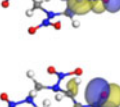
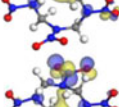
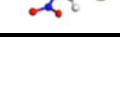

Temperature, K	HOMO	LUMO	$\Delta E(\text{L-H})$ , eV	RE, eV	$\Delta Q_{\text{Nitro,T}}$ , e
0			2.91	0	0
1000			2.39	2.51	0.080
2000			1.02	17.33	0.334
3000			0.77	17.63	0.074

distances of interest as shown in Fig. 9b, and listing all of the relevant data in Table 1, it is clear that all of the C–N bond lengths (denoted  $dI$ ,  $dII$ , and  $dIII$ , respectively, for the C–N bonds associated with NI, NII, and NIII) gradually decrease while the interatomic distances  $d1$ – $d12$  show different variations as the unit cell is compressed. There is also no obvious correlation between  $Q_{\text{nitro}}$  and the C–N bond lengths:  $Q_{\text{nitro}}$  fluctuates in a rather random manner as the bond lengths decrease. Therefore, we will turn our attention to the other atoms neighboring the nitro groups; i.e., we will consider the O··H distances. For all of the nitro groups, the plot of  $V/V_0$  versus  $Q_{\text{nitro}}$  shows a disparity (a jump or dip) between  $V/V_0 = 0.68$  and  $0.66$ : for NI,  $Q_{\text{nitro}}$  increases steeply; for NII and NIII, it decreases steeply. As shown in Table 1, the rapid increase in  $Q_{\text{nitro}}$  for NI can be attributed to a brief weakening of the

hydrogen bonding network that is induced by the rapid elongation of  $d1$  from 1.585 to 1.901 Å, despite the strengthening of the hydrogen bonding network caused by the shortening of  $d2$ ,  $d3$ , and  $d4$  by 0.069, 0.2, and 0.125 Å, respectively. Similarly, the rapid decreases in  $Q_{\text{nitro}}$  seen for NII and NIII are due to the significant shortening of  $d5$  and  $d6$  (by 0.307 and 0.354 Å, respectively) and  $d10$  and  $d11$  (by 0.15 and 0.115 Å, respectively). Meanwhile, it should be noted that the chemical bond torsion and electron delocalization that occur under compression can lead to jumps in the  $V/V_0$  versus  $Q_{\text{nitro}}$  plot. This lack of “smoothness” can also be seen in the plot of  $\Delta BG$  shown in Fig. 5b.

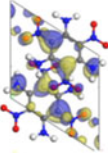
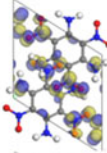
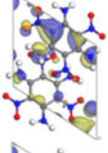
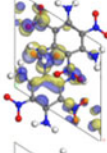
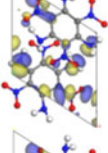
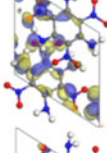
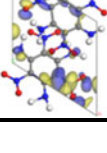
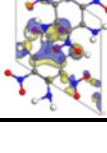
By the way, LDA indicates that there are some negative values of internal stress at the beginning of compression, and it gives lower internal stress values than GGA, such that

**Table 3** Distributions of frontier orbitals, energy gaps, relative energies, and changes in the average charge on a nitro group in an *NVT*-balanced HMX molecule at different temperatures

Temperature, K	HOMO	LUMO	$\Delta E(\text{L-H})$ , eV	RE, eV	$\Delta Q_{\text{Nitro,T}}$ , e
0			3.75	0	0
1000			2.53	9.26	0.186
2000			1.96	7.30	0.152
3000			1.71	8.32	0.151



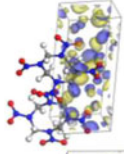
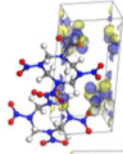
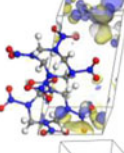
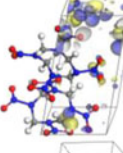
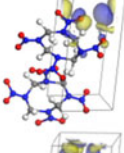
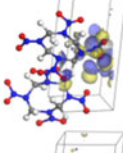
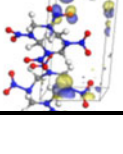
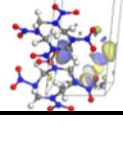
**Table 4** Distributions of frontier orbitals, energy gaps, relative energies, and the changes in the average charge on a nitro group in an *NVT*-balanced unit cell of TATB at different temperatures

Temperature, K	HOMO	LUMO	BG, eV	RE, eV	$\Delta Q_{\text{Nitro,T}}$ , e
0			2.50	0	0
1000			2.12	3.79	0.171
2000			1.55	17.66	0.682
3000			0.84	19.04	0.495

LDA underestimates the organic crystal volume compared to experimental results, whereas GGA overestimates them. Understandably, the unrelaxed state of compressed TATB results in more internal stress than the relaxed state, as shown in Figs. 5c and 6.

Moving on to analyze HMX, we first consider the charge transfer. Figure 10a shows that BLYP indicates a continuous and smooth charge transfer to the nitro groups, while both LDA and BPE indicate that the negative charges on the nitro groups first increase before they decrease for  $V/V_0 \geq 0.58$ .

**Table 5** Distributions of frontier orbitals, energy gaps, relative energies, and the changes in the average charge on a nitro group in an *NVT*-balanced unit cell of HMX at different temperatures

Temperature, K	HOMO	LUMO	BG, eV	RE, eV	$\Delta Q_{\text{Nitro,T}}$ , e
0			3.73	0	0
1000			2.14	12.77	0.318
2000			1.63	18.78	0.684
3000			1.50	16.76	0.471

This is different behavior to that seen for TATB. For TATB, the three DFT methods indicated that the negative charge increased, albeit with fluctuations, as the strain increased. This difference can be attributed to several reasons: for one thing, the atomic charges are sensitive to the method applied; for another, the nitro groups in HMX differ from those in TATB in terms of their abilities to attract electrons from their surrounding atoms during compression. Comparing the variations in  $\Delta Q_{\text{nitro}}$  shown in Figs. 5a and 10a, we can see that the nitro groups in TATB attract electrons much more strongly than those in HMX: when  $V/V_0=0.50$ , about  $-0.20e$  is transferred on average in TATB, while this figure is less than  $-0.01e$  in HMX. Thus, the charge transfer in perfectly crystalline HMX is not sensitive to compression. Two other observations support this: one is that BG decreases less with  $V/V_0$  for HMX (Fig. 10b) than for TATB (Fig. 5b); the other is the lower DOS for TATB than for HMX at a given strain (see Fig. 11). However, the trends in internal stress (as derived from the DFT calculations) for HMX (Fig. 10c) are similar to those seen for TATB (Fig. 5c).

#### Dynamic conditions

The dynamic behaviors of TATB and HMX at 1000, 2000, and 3000 K were simulated by performing ab initio MD calculations for their single gaseous molecules and unit cells, and the electronic structures of some randomly selected and dynamically balanced structures at different temperatures were recalculated to gain further insight into the charge transfer in these molecules.

We first considered the charge transfer in a single TATB molecule at different high temperatures. For all of the cases shown in Table 2, positive charge was transferred to the nitro groups, similar to the results obtained for static calculations of a single TATB molecule (see above). The sign of  $Q_{\text{nitro}}$  in TATB at high temperatures remains negative, based on the primary  $Q_{\text{nitro}}=-0.417e$  for the fully optimized TATB molecule. Also, as illustrated in Table 2, high temperatures break the symmetry of the TATB molecule and strongly deform it, changing the HOMO–LUMO distributions and decreasing the corresponding energy gaps  $\Delta E(L-H)$ , thus making the molecule much more energetic. Overall, high temperatures make the molecule unstable.

The results for a single HMX molecule (listed in Table 3) are mostly the same as those seen for a single TATB molecule. It is worth noting that the positive charge transferred to the nitro groups makes them more positively charged than the average charge on a nitro group ( $-0.112e$ ) in the fully optimized HMX molecule. If we compare the charges on the nitro groups in heated molecules of TATB and HMX, it is clear that TATB is more stable than HMX, based on the rule of nitro group charges [25].

Next, the charge transfer in perfectly crystalline TATB and HMX subjected to high temperatures is considered. As shown in Tables 4 and 5, the charge transfer in this case is very similar to that seen in the heated molecules, but it is very different from that seen when high pressures are applied. That is, positive charge is transferred *to* the nitro groups this time, not *from* the nitro groups (as occurs under high pressures). We think that high pressures are advantageous for shortening interatomic distances, transferring more electrons to nitro groups, and making them more negatively charged, while high temperatures lead to strong deformation of TATB and HMX molecules, which makes nitro groups less attractive to electrons.

#### Conclusions

Charge transfer in single molecules and the unit cells of the high-energy materials TATB and HMX under some extreme conditions, like high temperatures and high pressures, was simulated statically and dynamically. Three DFT methods—LDA, BLYP, and BPE—were employed for the simulations. High temperatures were found to encourage negative charge transfer from the nitro groups in single molecules and unit cells of these two molecules in both static and dynamic calculations, while the reverse (and more complicated) behavior was seen when high uniform pressures were applied. That is, for TATB, all of the DFT calculations showed negative charge transfer to the nitro groups when the pressure was increased; while for HMX, BLYP calculations indicated continuous negative charge transfer to the nitro groups, while LDA and BPE calculations pointed to initial negative charge transfer to the nitro groups, followed by negative charge transfer from these groups when the pressure exceeded a certain value. BLYP calculations for an unrelaxed and compressed unit cell of TATB indicated negative charge transfer from the nitro groups.

We believe that charge transfer, which is essentially electron transfer, is related to the relative positions of the atoms in the system of interest. Different DFT methods sometimes give different variations in charge transfer because they can give different electronic structures under extreme conditions.

**Acknowledgments** Dr. Zhang greatly appreciates the financial support from the Science and Technology Fund of China Academy of Engineering Physics (CAEP) (2011A0302014) and the National Natural Science Foundation of China (21173199 and 11072225).

#### References

1. LANL (2012) The rapidly changing landscape for MaRIE. [http://www.lanl.gov/science/NSS/issue2\\_2010/story5.shtml](http://www.lanl.gov/science/NSS/issue2_2010/story5.shtml)
2. Kohno Y, Hiyoshi RI, Yamaguchi Y, Matsumoto S, Koseki A, Takahashi O, Yamasaki K, Ueda K (2009) Molecular dynamics

- studies of the structural change in 1,3-diamino-2,4,6-trinitrobenzene (DATB) in the crystalline state under high pressure. *J Phys Chem A* 113:2551–2560
- Wu CJ, Yang LH, Fried LE, Quenneville J, Martinez TJ (2003) Electronic structure of solid 1,3,5-triamino-2,4,6-trinitrobenzene under uniaxial compression: possible role of pressure-induced metallization in energetic materials. *Phys Rev B* 67:235101
  - Manaa MR, Reed EJ, Fried LE, Goldman N (2009) Nitrogen-rich heterocycles as reactivity retardants in shocked insensitive explosives. *J Am Chem Soc* 131:5483–5487
  - Manaa MR, Fried LE, Melius CF, Elstner M, Frauenheim TJ (2002) Decomposition of HMX at extreme conditions: a molecular dynamics simulation. *Phys Chem A* 106:9024–9029
  - Chang J, Lian P, Wei DQ, Chen XR, Zhang QM, Gong ZZ (2010) Thermal decomposition of the solid phase of nitromethane: ab initio molecular dynamics simulations. *Phys Rev Lett* 105:188302
  - Strachan A, van Duin ACT, Chakraborty D, Dasgupta S, Goddard WA (2003) Shock waves in high-energy materials: the initial chemical events in nitramine RDX. *Phys Rev Lett* 91:098301
  - Furnish MD, Russell TP, White CT (2005) Shock compression of condensed matter. AIP, New York
  - Nomura K, Kalia RK, Nakano A, Vashishta P (2007) Reactive nanojets: nanostructure-enhanced chemical reactions in a defected energetic crystal. *Appl Phys Lett* 91:183109
  - Zybin SV, Goddard WA, Xu P, van Duin ACT, Thompson AP (2010) Physical mechanism of anisotropic sensitivity in pentaerythritol tetranitrate from compressive-shear reaction dynamics simulations. *Appl Phys Lett* 96:081918
  - Nomura K, Kalia RK, Nakano A, Vashishta P, van Duin ACT, Goddard WA (2007) Dynamic transition in the structure of an energetic crystal during chemical reactions at shock front prior to detonation. *Phys Rev Lett* 99:148303
  - Boyd S, Murray JS, Politzer P (2009) Molecular dynamics characterization of void defects in crystalline (1,3,5-trinitro-1,3,5-triazacyclohexane). *J Chem Phys* 131:204903
  - Piquemal JP, Marquez A, Parisel O, Prettre CG (2005) A CSOV study of the difference between HF and DFT intermolecular interaction energy values: the importance of the charge transfer contribution. *J Comput Chem* 26:1052–1062
  - Zhao GJ, Han KL (2008) Time-dependent density functional theory study on hydrogen-bonded intramolecular charge-transfer excited state of 4-dimethylamino-benzonitrile in methanol. *J Comput Chem* 29:2010–2017
  - Perdew JP, Wang Y (1992) Accurate and simple analytic representation of the electron-gas correlation energy. *Phys Rev B* 45:13244
  - Liu Y, Tuckerman ME (2000) Generalized Gaussian moment thermostatting: a new continuous dynamical approach to the canonical ensemble. *J Chem Phys* 112:1685–1690
  - Verlet L (1967) Computer “experiments” on classical fluids. I. Thermodynamical properties of Lennard–Jones molecules. *Phys Rev* 59:98
  - Byrd EFC, Scuseria GE, Chabalowski CF (2004) An ab initio study of solid nitromethane, HMX, RDX, and CL20: successes and failures of DFT. *J Phys Chem B* 108:13100–13106
  - Byrd EFC, Rice BM (2008) Ab initio study of compressed 1,3,5,7-tetranitro-1,3,5,7-tetraazacyclooctane (HMX), cyclotrimethylene-trinitramine (RDX), 2,4,6,8,10,12-hexanitrohexaazaisowurzitane (CL-20), 2,4,6-trinitro-1,3,5-benzenetriamine (TATB), and pentaerythritol tetranitrate (PETN). *J Phys Chem C* 111:2787–2796
  - Delley B (1990) An all-electron numerical method for solving the local density functional for polyatomic molecules. *J Chem Phys* 92:508–517
  - Delley B (2000) From molecules to solids with the DMol<sup>3</sup> approach. *J Chem Phys* 113:7756–7764
  - Accelrys Inc. (2009) Materials Studio 5.0. Accelrys Inc., San Diego
  - Zhang C, Shu Y, Huang Y, Zhao X, Dong H (2005) Investigation of correlation between impact sensitivities and nitro group charges in nitro compounds. *J Phys Chem B* 109:8978–8983
  - Kuklja MM, Rashkeev SN (2007) Shear-strain-induced structural and electronic modifications of the molecular crystal 1,1-diamino-2,2-dinitroethylene: slip-plane flow and band gap relaxation. *Phys Rev B* 75:104111
  - Zhang C (2009) Review of the establishment of nitro group charge method and its applications. *J Hazard Mater* 161:21–29